The Black Hole Universe (BHU) from a FLRW cloud

Enrique Gaztanaga

A Black Hole Universe (BHU) out of a FLRW cloud

Enrique Gaztañaga[a,b]

[a]Institute of Space Sciences (ICE,CSIC), , Bellaterra, 08193, Barcelona, Spain
[b]Institut d Estudis Espacials de Catalunya (IEEC), , Barcelona, 08034, Barcelona, Spain

Abstract

A FLRW cloud is a solution of classical General Relativity (GR) were a homogeneous fluid of fixed mass M collapses in a free fall, following a radial geodesic $R(\tau)$ of the FLRW metric. This solution can be used to model the interior of a Black Hole (BH) with regular matter/radiation, without the need of negative pressure or surface terms. We propose that our Universe emerged from such a FLRW cloud with mass $M \simeq 5 \times 10^{22} M_{\odot}$ that collapsed 25 Gyrs ago inside its own event horizon $r_S = 2GM$. The resulting BH had a very low density, so the collapse continues inside for 11 Gyrs. When it reaches neutron star density it explodes, like a Supernova, into the hot Big Bang expansion that we observe today. Such BHU expansion is trapped inside $r_S = 2GM$, which acts like a cosmological constant $\Lambda = 3/r_S^2$. The BHU expansion follows $R \simeq [r_H^2 r_S]^{1/3}$ so a large fraction of M is outside its Hubble radius $r_H = H^{-1}$. This solves the horizon and structure formation problems. Thus, the BHU model does not need Dark Energy or Inflation, yet it can be tested using current Cosmic maps because the observable Universe today is larger than r_S.

Keywords: Cosmology, Dark Energy, General Relativity, Black Holes, Dark Matter
PACS: 0000, 1111
2000 MSC: 0000, 1111

1. Introduction

The Big Bang (BB), Dark Energy (DE), Λ, inflation, DM and BHs are puzzles we don't yet understand at any fundamental level. The corresponding GR solutions, e.g. FLRW or Schwarzschild (SW) metrics, involve non physical singularities. Singularity theorems are sometimes interpreted as an indication that a new theory of (Quantum) Gravity might be needed to understand these puzzles. But this is far from settle (see [1]). May be we don't need a new theory of Gravity but just a better model. That a non singular version of such solutions exist is clear from direct observations. Singularities often represent a simple approximation to a more complex physical solution. Our goal is to look for a better approximation within GR to understand these puzzles at a more fundamental level. We elaborate on a well known example of non singular BH: a Bubble Universe. This is a domain wall that connects a region of true and false vacuum, with de Sitter (dS) space inside. These solutions are not very appealing because they have no matter or radiation anywhere, except in a surface term or bubble, required to glue the dS and SW discontinuity (e.g. see [2, 3, 4]). The BHU proposal presented here can be thought as a type of Bubble Universe with a FLRW interior (including regular matter and radiation) and no bubble or surface term. The empty space outside is just a local approximation, which is used to describe isolated BHs, like in the SW metric. In a more realistic situation we can interpret the BH solution to exist inside another FLRW background [5].

The BB with inflation is the standard cosmological model that we use to interpret observations such as BAO, SN, CMB and LSS. This is despite the fact that we have no idea of how the BB or inflation started. For the same reason, we don't need a particular formation mechanism to consider the BHU as a possible alternative to the BB and BH paradigms. In §5, we give some ideas about how a BHU could form. But our scope and focus here is not so much on the formation mechanism itself but to show that some new solutions exist that can help us understanding the above puzzles at a more fundamental level.

A Schwarzschild BH metric (BH.SW) represents a singular object of mass M. The BH event horizon $r_S \equiv 2GM$ prevent us from interacting with the inside (which makes BHs good candidates for DM). Physically, a singular point does not make any sense. What is the metric inside? What happens when matter or BHs merge? Do BHs grow and co-evolve with galaxies (e.g. [6])? Do observed BH form in stellar collapse or are they seeded by primordial BHs? How do primordial BH form (e.g. [7])? Most of these modelings assume the BH.SW solution, but can we actually answer any of these questions if we do not have a physical model for the BH interior?

Here, we look for an alternative solution to the BH.SW interior, defined as a non singular object of size r_S which reproduces the BH.SW metric for the outside $r > r_S$. A physical BH of size $r = r_S$ and mass M, has a density:

$$\rho_{BH} = \frac{M}{V} = \frac{3r_S^{-2}}{8\pi G} = \frac{3M^{-2}}{32\pi G^3} \,. \tag{1}$$

The BH interior can not be made out of regular matter or radiation because according to GR a perfect fluid with mass M has a minimal radius ([8]):

$$R > 9/8 r_S. \tag{2}$$

But objects with mass and sizes matching r_S have been observed.

What is inside a BH then? The highest known density for a stellar object is that of a Neutron star, which has the density of an atomic nucleus, but is still a few times larger than r_S. To achieve such a high density for a perfect fluid, the radial pressure inside a BH needs to be negative ([9] and references therein). Cosmologist are used to this type of fluids, which are called Quintessence, Inflation or Dark Energy (DE). So, could the inside of a BH be DE? [10] have argued that the same DE repulsive force that causes cosmic acceleration could also prevent the BH singular collapse.

We find a new solution to these questions, which we call the BHU (for $R < r_S$) or FLRW cloud (for $R > r_S$). We will also explore the idea that our Universe corresponds to such BHU solution. As the universe expands H tends to H_Λ which corresponds to a trapped surface $r_\Lambda = 1/H_\Lambda$, just like the event horizon of a BH. Moreover, the density of our universe in that limit is $\rho = 3H_\Lambda^2/8\pi G$ which exactly corresponds to that of a BH, in Eq.1 for $r_S = r_\Lambda$. In fact, the Hubble Horizon $r_H = 1/H$ also has this property. This is not just a coincidence as advocated by some scientist ([11, 12]). It directly indicates that we actually live inside a very massive physical BH. It also tells us what is the metric inside a BH. Our Universe is the only object whose interior we know and has the density of a BH. And the metric that we observe is the FLRW metric. We will explicitly show that such BHU or FLRW cloud is a solution to classical GR.

The idea that the universe might be generated from the inside of a BH is not new and has extensive literature (see [13, 14] and references therein) which mostly focused in dS metric with a dual role of the BH interior and an approximation for our universe. Many of the formation mechanisms involve some modifications or extensions of GR, often motivated by quantum gravity or string theory. This is what we try to avoid here, following the arguments in [15]. There are also some simple scalar field $\varphi(x)$ examples (e.g. [16]) which presented models within the scope of a classical GR and classical field theory with a false vacuum (FV) interior similar to our BH.fv solution here. These models have been questioned using no-go theorems, such us that by [17], that state that no smooth solution to $\varphi(x)$ can interpolate between dS and SW space. But this is not an issue for our solution for three reasons. First, the external asymptotic space is really SW+dS or FLRW (a BH is a perturbation within a FLRW metric), where solutions do exist (e.g. [18]). Second, we do not need $\varphi(x)$ to smoothly transit between metrics: $\varphi(x)$ is trapped in a FV, which is discontinuous by nature, as shown in the Bubble Universes (e.g. see [2, 3, 4]). Finally, we do not actually need a scalar field or ρ_Λ to have a BHU solution. We just need the interior of the BH to follow a FLRW geodesic, which results in no bubble or surface terms.

Several authors before have grasped the idea or speculated that the FLRW metric could be the interior of a BH ([19, 20, 21, 22]). But these previous solution were incomplete ([12]) or outside classical GR. [23] showed, independently from us, that a dust filled FLRW metric can be joined to an outside BH.SW metric, in good agreement with what we find in §4.

Our BHU solution sounds similar, but is quite different from that of [24], who speculated that all final (e.g. BH) singularities 'bounce' or tunnel to initial singularities of new universes. Here we propose the opposite, that such mathematical singularities are not needed to explain the physical world. As stated by [25], the concept of physical infinity is not a scientific one if science involves testability by either observation or experiment. The BHU model can avoid the initial causal and entropy paradoxes ([26, 27]) because our universe could start as a FLRW collapsing cloud, and entropy decreases during the collapse because of gravity.

In §2 we present the GR field equations of a perfect fluid for homogeneous solutions: a FV and an expanding FLRW universe. We also give a brief introduction to the general case of solutions with spherical symmetry in physical SW coordinates. The FLRW solution can also be expressed as in-homogeneous in these SW coordinates. This duality is a key ingredient to find and interpret our new solutions for a BH interior in §3. In §4 and §5 we study the junction of the BHU and FLRW cloud solutions and its formation. We also discuss how these solutions apply both to BHs and to our Universe. We end with a summary and a discussion of observational windows to test the BHU.

2. Some simple solutions

Given the Einstein-Hilbert action ([28, 29, 30, 31]):

$$S = \int_{V_4} dV_4 \left[\frac{R - 2\Lambda}{16\pi G} + \mathcal{L} \right], \tag{3}$$

where $dV_4 = \sqrt{-g} d^4x$ is the invariant volume element, V_4 is the volume of the 4D spacetime manifold, $R = R^\mu_\mu = g^{\mu\nu} R_{\mu\nu}$ is the Ricci scalar curvature and $\mathcal{L}$ the Lagrangian of the energy-matter content. We can obtain Einstein's field equations (EFE) for the metric field $g_{\mu\nu}$ from this action by requiring S to be stationary $\delta S = 0$ under arbitrary variations of the metric $\delta g^{\mu\nu}$. The solution is ([32, 30, 31]):

$$G_{\mu\nu} + \Lambda g_{\mu\nu} = 8\pi G \, T_{\mu\nu} \equiv -\frac{16\pi G}{\sqrt{-g}} \frac{\delta(\sqrt{-g}\mathcal{L})}{\delta g^{\mu\nu}}, \tag{4}$$

where $G_{\mu\nu} \equiv R_{\mu\nu} - \frac{1}{2} g_{\mu\nu} R$ and $\mathcal{L}$ is the matter Lagrangian. For perfect fluid in spherical coordinates:

$$T_{\mu\nu} = (\rho + p) u_\mu u_\nu + p g_{\mu\nu} \tag{5}$$

where u_ν is the 4-velocity ($u_\nu u^\nu = -1$), ρ, and p are the energy-matter density and pressure. This fluid is made of several components, each with a different equation of state $p = \omega\rho$.

Eq.4 requires that boundary terms vanish (e.g. see [33, 34, 31]). Otherwise, we need to add a Gibbons-Hawking-York (GHY) boundary term [35, 36, 37] to the action:

$$S = \int_{V_4} dV_4 \left[\frac{R - 2\Lambda}{16\pi G} + \mathcal{L} \right] + \frac{1}{8\pi G} \oint_{\partial V_4} d^3y \sqrt{-h} \, K. \tag{6}$$

where K is the trace of the extrinsic curvature at the boundary ∂V_4 and h is the induced metric. We will show explicitly in §4.2 that the GHY boundary results in a Λ term when the evolution happens following a FLRW metric inside an expanding BH event horizon. To cancel the GHY term we need $r_\Lambda = r_S$. That Λ is a GHY term was propose in [38] and has also been later interpreted as a boundary entropy term by [39, 40, 41].

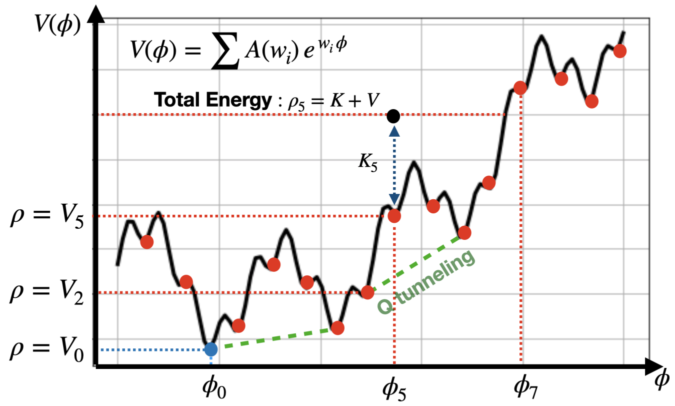

Figure 1: The potential $V(\phi)$, of a classical scalar field $\phi(x)$, made of the superposition of plane waves. A configuration with total energy: $\rho_5 = K_5 + V_5$ (black dot at ϕ_5) can loose its kinetic energy K_5 during expansion (e.g. a supernova explosion or a expanding background) due to Hubble damping and relax into one of the static ($K = 0$) ground state (or FV) $\rho_5 = V_5 \equiv V(\phi_5)$ (red dots). This can generate a Black Hole (BH.fv) and regular matter from reheating. Each FV has an energy excess $\Delta_i \equiv V_i - V_0$ over the true vacuum at V_0 (blue dot). Quantum tunneling (dashed lines) could allow ϕ to jump between FV, resulting in BH evaporation and new matter/radiation.

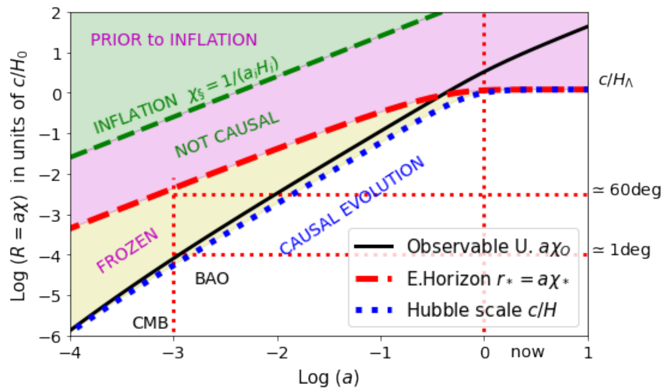

Figure 2: Physical radial coordinate $R = a(\tau)\chi$ in units of c/H_0 as a function of cosmic time a for a flat $\Omega_\Lambda = 0.75$ FLRW metric. The Hubble horizon c/H (blue dotted line), is compared to the observable universe r_o in Eq.18 (continuous line) and the FLRW Event Horizon $r_* = a\chi_*$ in Eq.17 (dashed red line), which here is smaller than the primordial causal boundary of inflation $\chi_{\S}$ (dashed green line). Scales larger than $a\chi_{\S}$ are prior to inflation. Scales larger than r_* are causally disconnected (magenta shading). Scales smaller than r_* but larger than c/H are dynamically frozen (yellow shading). At $a \simeq 1$ (now) the Hubble horizon reaches our event horizon $a\chi_* = c/H_\Lambda$. Table 1 gives a summary of the different scales presented.

2.1. Scalar field in curved space-time

Consider a minimally coupled scalar field $\varphi = \varphi(x_\alpha)$ with:

$$\mathcal{L} \equiv K - V = -\frac{1}{2}\partial_\alpha\varphi\partial^\alpha\varphi - V(\varphi) \tag{7}$$

The Lagrange equations are: $\bar{\nabla}^2\varphi = \partial V/\partial\varphi$. We can estimate $T_{\mu\nu}(\varphi)$ from its definition in Eq.4 to find [30]:

$$T_{\mu\nu}(\varphi) = \partial_\mu\varphi\partial_\nu\varphi + g_{\mu\nu}(K - V) \tag{8}$$

comparing to Eq.5:

$$\rho = K + V \quad ; \quad p = |K| - V \tag{9}$$

In general we can have $p_\parallel \neq p_\perp$ for non canonical scalar fields (see Eq.5 in [42] for further details). The stable solution corresponds to $p = -\rho \equiv -\rho_{vac}$:

$$\bar{\nabla}^2\varphi = \partial V/\partial\varphi = 0 \quad ; \quad \rho \equiv \rho_{vac} = -p = V(\varphi) = V_i \tag{10}$$

where φ is trapped in the true minimum V_0 or some false vacuum (FV) state $V_i = V_0 + \Delta$. The situation is illustrated in Fig.1.

2.2. The FLRW metric in comoving coordinates

The flat FLRW metric in comoving coordinates $\xi^\alpha = (\tau, \chi, \theta, \delta)$, corresponds to an homogeneous and isotropic space:

$$ds^2 = f_{\alpha\beta}d\xi^\alpha d\xi^\beta = -d\tau^2 + a(\tau)^2\left[d\chi^2 + \chi^2 d\Omega\right] \tag{11}$$

where we have introduced the solid angle: $d\Omega^2 = d\theta^2 + \sin\theta^2 d\delta^2$. The scale factor, $a(\tau)$, describes the expansion/contraction as a function of comoving or cosmic time τ (proper time for a comoving observer). For a comoving observer, $u = 0$, the time-radial components of Eq.5 are:

$$\begin{pmatrix} T_{00} & T_{10} \\ T_{01} & T_{11} \end{pmatrix} = \begin{pmatrix} \rho(\tau) & 0 \\ 0 & p(\tau)a^2 \end{pmatrix} \tag{12}$$

and the solution to EFE in Eq.4 is then:

$$3\left(\frac{\ddot{a}}{a}\right) = R_{\mu\nu}u^\mu u^\nu = \Lambda - 4\pi G(\rho + 3p) \tag{13}$$

$$H^2 \equiv \left(\frac{\dot{a}}{a}\right)^2 = H_0^2\left[\Omega_m a^{-3} + \Omega_R a^{-4} + \Omega_\Lambda\right] \tag{14}$$

$$\rho_\Lambda \equiv \rho_{\text{vac}} + \frac{\Lambda}{8\pi G} \tag{15}$$

$$\rho_c \equiv \frac{3H^2}{8\pi G} \quad ; \quad \Omega_X \equiv \frac{\rho_X}{\rho_c(a=1)} \tag{16}$$

where Ω_m (or ρ_m) represent the matter density today ($a = 1$), Ω_R is the radiation, ρ_{vac} represents vacuum energy: $\rho_{\text{vac}} = -p_{\text{vac}} = V(\varphi)$ in Eq.10, and $\rho_\Lambda = -p_\Lambda$ is the effective cosmological constant density. Note that Λ (the raw value) is always constant, but ρ_Λ (effective value) can change if ρ_{vac} changes. Given $\rho(\tau)$ and $p(\text{‘}tau)$ we can use the above equations to find $a(\tau)$.

2.3. The FLRW metric as a Black Hole

Observations show that the expansion rate today is dominated by ρ_Λ. This indicates that the FLRW metric lives inside a trapped surface $r_\Lambda \equiv 1/H_\Lambda = (8\pi G\rho_\Lambda/3)^{-1/2}$, which behaves like the interior of a BH. To see this, consider outgoing radial null geodesic (the Event Horizon at τ, [43]):

$$r_* \equiv a\chi_* = a\int_\tau^\infty \frac{d\tau}{a(\tau)} = a\int_a^\infty \frac{d\ln a}{aH(a)} < \frac{1}{H_\Lambda} \equiv r_\Lambda \tag{17}$$

where $\chi_*(a)$ is the corresponding comoving scale. For small a the value of χ_* is fixed to a constant $\chi_* \simeq 3r_\Lambda$. Thus, the physical trapped surface radius r_* increases with time. As we approach $a \simeq 1$ the Hubble rate becomes constant and r_* freezes to a constant value $r_* = r_\Lambda$ This is shown as a red dashed line in Fig.2. No signal from inside r_* can reach outside, just like in the interior of a BH. In fact, according to Birkhoff theorem (see [44]), the metric outside should be exactly that of the BH.SW in the limit of empty outside space. So the FLRW metric is a BH:SW from the outside with $r_S = r_\Lambda$. This breaks homogeneity (on scales larger than r_Λ), but this is needed if we want causality. Homogeneity is inconsistent with a causal origin.

The causal boundary of inflation $\chi_\S$ (shown as green dashed line) corresponds to the particle horizon during inflation $\chi_\S = c/(a_i H_i)$ or the Hubble horizon $1/H_i$ when inflation begins a_i. We can in principle have that $\chi_\S > \chi_*$, as shown in the figure. But why should there be two separate causal scales?

The observable universe or particle horizon is:

$$r_o = a \int_{a_e}^{a} \frac{d\ln a}{aH(a)} \tag{18}$$

where a_e is either $a_e = 0$ (in models without inflation) or the scale factor when inflation ends. For $\Omega_\Lambda \simeq 0.7$, the particle horizon today is $r_o \simeq 3.26c/H_0$, which is larger than r_Λ as shown in Fig.2. This shows that, observers like us are trapped inside $r_* = a\chi_*$ but can nevertheless observe what happened outside. If we look back to the CMB maps ($a \simeq 10^3$) we can see frozen BAO scales (outsisde the Hubble scale $1/H$ at $\theta \simeq 1$deg. on the sky) but also scales outside our Event Horizon r_* ($\theta \simeq 60$deg. on the CMB sky) [45, 38, 46, 47, 48].

2.4. Spherical symmetry in physical coordinates

The most general shape for a metric with spherical symmetry in physical or SW coordinates (t, r, θ, δ) can be writen as:

$$ds^2 = g_{\mu\nu}dx^\mu dx^\nu = -(1+2\Psi)dt^2 + \frac{dr^2}{1+2\Phi} + r^2 d\Omega^2 \tag{19}$$

where $\Psi(t, r)$ and $\Phi(t, r)$ are the two gravitational potentials. The Weyl potential Φ_W is the geometric mean of the two:

$$(1+2\Phi_W)^2 = (1+2\Phi)(1+2\Psi) \tag{20}$$

Ψ describes propagation of non-relativist particles and Φ_W the propagation of light. For $p = -\rho$ we have $\Psi = \Phi = \Phi_W$. Eq.19 can also be used to describe the BH.SW solution (or any other solution) as a perturbation ($2|\Phi| < 1$) around a FLRW background:

$$ds^2 \simeq -(1+2\Psi)dt^2 + (1-2\Phi)a^2 d\chi^2 + a^2\chi^2 d\Omega^2 \tag{21}$$

where $r = a(\tau)\chi$ and $t \simeq \tau$. The same result follows from perturbing the FLRW metric in Eq.11.

Solutions to EFE for Eq.19 are well known, e.g. see Eq.(7.51) in [31]. For a static perfect fluid BH with arbitrary $\rho(r)$ inside r_S and empty space ($\Lambda = 0$) outside, we have $G^0_0 = -8\pi G\rho(r)$. This can be solved using $m(r)$:

$$\Phi(r) = -\frac{Gm(r)}{r} = -\frac{G}{r}\int_0^r \rho(r)\, 4\pi r^2 dr \tag{22}$$

so the interior $r < r_S$ of a BH has:

$$\Phi(r) = \begin{cases} -GM/r & \text{for } \rho(r) = M\,\delta_D(r) \\ -\frac{1}{2}(r/r_0)^2 & \text{for } \rho(r) = \rho_0 \equiv \frac{3}{8\pi r_0^2} \end{cases} \tag{23}$$

$\Psi(r)$ depends on G^1_1 and $p(r)$. For $p = -\rho$ we have $G^0_0 = G^1_1$ and the general solution with $\Lambda \neq 0$ is:

$$\Phi = \Psi = -\frac{Gm(r)}{r} - \frac{\Lambda r^2}{6} \tag{24}$$

The remaining EFE in Eq.4 are $G^2_2 = G^3_3$ and correspond to energy conservation $\nabla_\mu T^\mu_\nu = 0$. For a comoving observer $u = 0$ in a perfect fluid of Eq.5:

$$\partial_t\rho = -\frac{\rho+p}{1+2\Phi}\,\partial_t\Phi. \;\; ; \;\; \partial_r p = \frac{\rho+p}{1+2\Psi}\,\partial_r\Psi \tag{25}$$

Note how $\rho = -p$ results in constant ρ and p in time and everywhere, but with a discontinuity at $2\Phi = 2\Psi = -1$. This means that ρ and p could be constant but different in both sides of $2\Phi = 2\Psi = -1$. This will be addressed with the study of junction conditions in §4).

Empty space ($\rho = p = \rho_\Lambda = 0$) in Eq.24 results in the BH.SW metric:

$$2\Phi = 2\Psi = -2GM/r \equiv -r_S/r \tag{26}$$

There is a trapped surface at $r = r_S$ ($2\Phi = -1$). Outgoing radial null geodesics cannot leave the interior of r_S, while incoming ones can cross inside. The solution to Eq.24 for $\rho = p = M = 0$, but $\rho_\Lambda \neq 0$ results in deSitter (dS) metric:

$$2\Phi = 2\Psi = -r^2/r_\Lambda^2 \equiv -r^2 H_\Lambda^2 = -r^2 8\pi G\rho_\Lambda/3 \tag{27}$$

where ρ_Λ is the effective density: $\rho_\Lambda = \Lambda/(8\pi G) + V(\varphi)$. We can immediately see that this solution is the same as the interior of a BH with constant density in Eq.23 with $\rho_0 = \rho_\Lambda$.

dS metric corresponds to the surface of a hypersphere of radius r_Λ in a flat spacetime with an extra spatial dimension (see Appendix A). This has a constant positive Ricci curvature $R = 4\Lambda$ and a finite volume inside r_Λ. As in the BH.SW metric, dS metric also has a trapped surface at $r = r_\Lambda$ ($2\Phi = -1$). Radial null events ($ds^2 = 0$) connecting $(0, r_0)$ with (t, r) follow:

$$r = r_\Lambda \frac{r_\Lambda + r_0 - (r_\Lambda - r_0)e^{-2t/r_\Lambda}}{r_\Lambda + r_0 + (r_\Lambda - r_0)e^{-2t/r_\Lambda}} \tag{28}$$

so that it takes $t = \infty$ to reach $r = r_\Lambda$ from any point inside. The BH.SW metric is singular at $r = 0$, while dS is singular at $r = \infty$. But note that this singularity can not be reached from the inside because of the trapped surface at r_Λ in Eq.28. The inside observer is trapped, like in the FLRW case. Both metrics are equivalent for $H = H_\Lambda$ (see [49, 50]) which explains why the dS metric reproduces primordial inflation in comoving coordinates. For M and ρ_Λ constant, the solution to Eq.24 is:

$$2\Phi = 2\Psi = -r^2 H_\Lambda^2 - r_S/r, \tag{29}$$

which corresponds to dS-SW (dSW) metric, a BH.SW within a dS background. Solution of a BH inside a FLRW metric also exist (e.g see [5]). Here we will show that GR solutions also exit for a FLRW inside a BH (or inside a larger FLRW metric).

We also consider a generalization of dS metric, which we call dS extension (dSE), which is just a recast of the general case:

$$2\Phi(t, r) \equiv -r^2 H^2(t, r) \equiv -r^2/r_H^2 \tag{30}$$

Table 1 shows a summary of notation and metrics considered in this paper.

Table 1: Some notation used in this paper.

Notation	name	comment
$r_\Lambda = 1/H_\Lambda$	deSitter (dS) Event Horizon	$3H_\Lambda^2 = 8\pi G\rho_\Lambda$, Eq.27
$-2\Phi = r^2 H_\Lambda^2$	dS metric Eq.27	static, inside BH.fv
$r_S = 2GM$	BH Event Horizon	$\rho_{BH}(r_\Lambda) = \rho_\Lambda$, Eq.1
$-2\Phi = r_S/r$	Schwarzschild (SW) metric	BH.SW, outside BHU, Eq.26
$-2\Phi = r_S/r + r^2 H_\Lambda^2$	dSW = dS-SW	static, outside BHU, Eq.29
$-2\Phi = \begin{cases} r_S/r & \text{for } r > r_S \\ r^2 H_\Lambda^2 & \text{for } r < r_S \end{cases}$	False Vacuum or BH.fv	frozen BHU in Eq.36
$r_* = a\chi_*(\tau) = a\int_\tau^\infty \frac{d\tau}{a(\tau)}$	FLRW Event Horizon	Outgoing null geodesic Eq.17
$r_H = 1/H$	Hubble Horizon	$r > r_H$ frozen Fig.2
$-2\Phi = r^2 H^2$	dSE= dS Extension Eq.30	FLRW or BH.u interior Eq.33
$R = \left[r_H^2 r_S\right]^{1/3}$	BHU Junction Eq.39, Eq.51	Null geodesic: $R = r_*$ Eq.C.5
$-2\Phi = \begin{cases} r_S/r & \text{for } r > R \\ r^2 H^2 & \text{for } r < R \end{cases}$	FLRW cloud for $R > r_S$	BH.u for $R < r_S$, Eq.38
$r_o = a\chi_o = a\int_0^\tau \frac{d\tau}{a(\tau)}$	Observable Universe Eq.18	Particle Horizon today $r_o > r_\Lambda$
$r_\S = a(\tau)\chi_\S = a(\tau)\chi_*$	Causal Boundary Eq.45	for Inflation: $\chi_\S = \chi_* = (a_i H_i)^{-1}$

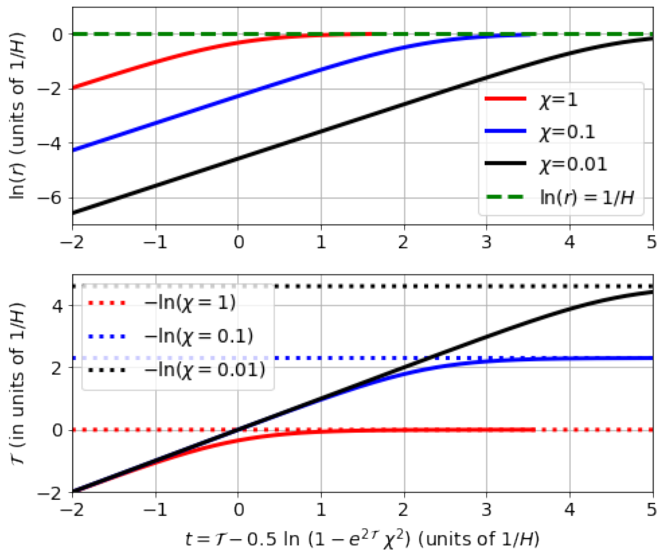

Figure 3: Logarithm of physical radius $r = a(\tau)\chi$ (top) and comoving time τ (bottom) as a function of SW time t in Eq.34 for $a(\tau) = e^{\tau H_\Lambda}$ and different values of χ. All quantities are in units of $1/H_\Lambda$. For early time or small χ: $\tau \simeq t$. A fix χ acts like an Horizon: as $t \Rightarrow \infty$ we have $\tau \Rightarrow -\ln\chi$ (dotted), which freezes inflation to: $r = a\chi \Rightarrow e^{-\ln(H_\Lambda\chi)}\chi = 1/H_\Lambda$ (dashed).

3. Some new solutions

Here we consider some additional solutions with spherical symmetry which are simple variations of the previous well known cases in Table 1.

3.1. The FLRW metric in physical coordinates

Consider a change of variables from $x^\mu = [t, r]$ to comoving coordinates $\xi^\nu = [\tau, \chi]$, where $r = a(\tau)\chi$ and angular variables (θ, δ) remain the same. The metric $g_{\mu\nu}$ in Eq.19 transforms to $f_{\alpha\beta} = \Lambda_\alpha^\mu \Lambda_\beta^\nu g_{\mu\nu}$, with $\Lambda_\nu^\mu \equiv \frac{\partial x^\mu}{\partial \xi^\nu}$. If we use:

$$\Lambda = \begin{pmatrix} \partial_\tau t & \partial_\chi t \\ \partial_\tau r & \partial_\chi r \end{pmatrix} = \begin{pmatrix} (1+2\Phi_W)^{-1} & arH(1+2\Phi_W)^{-1} \\ rH & a \end{pmatrix} \tag{31}$$

with $2\Phi = -r^2 H^2$ and arbitrary $a(\tau)$ and Ψ, we find:

$$f_{\alpha\beta} = \Lambda^T \begin{pmatrix} -(1+2\Psi) & 0 \\ 0 & (1+2\Phi)^{-1} \end{pmatrix} \Lambda = \begin{pmatrix} -1 & 0 \\ 0 & a^2 \end{pmatrix} \tag{32}$$

In other words, these two metrics are the same:

$$-(1+2\Psi)dt^2 + \frac{dr^2}{1 - r^2 H^2} = -d\tau^2 + a^2 d\chi^2 \tag{33}$$

dSE metric in Eq.30 with $2\Phi = -r^2 H^2$ corresponds to the FLRW metric with $H(t, r) = H(\tau)$: this is a hypersphere of radius r_H that tends to r_Λ (see Appendix A). This frame duality can be understood as a Lorentz contraction $\gamma = 1/\sqrt{1 - u^2}$ where the velocity u is given by the Hubble-Lemaitre law: $u = Hr$. An observer in the SW frame, not moving with the fluid, sees the moving fluid element $ad\chi$ contracted by the Lorentz factor γ: $ad\chi \Rightarrow \gamma dr$. For constant H, the FLRW metric corresponds the interior of a BH with constant density in Eq.23. A Lorentz factor γ also explains $d\tau = \gamma^{-1} dt$ as time dilation.

Given $a(\tau)$, we can find Ψ and $\tau = \tau(t, r)$. For $a(\tau) = e^{\tau H_\Lambda}$ we have $2\Psi = 2\Phi = -r^2 H_\Lambda^2$ and (see [49, 51]):

$$t = t(\tau, \chi) = \tau - \frac{1}{2H_\Lambda} \ln\left[1 - H_\Lambda^2 a^2 \chi^2\right], \tag{34}$$

which reproduces dS metric. In comoving coordinates the metric is inflating exponentially: $a = e^{\tau H_\Lambda}$, while in physical coordinates it is static. Fig.3 illustrates how this is possible and shows how $\tau = \tau(t, r)$ freezes (see [50] for some additional discussion). Note also how $\partial_\tau t = (1 + 2\Phi_W)^{-1}$ in Eq.31 for $2\Phi_W = -r^2 H^2$ is the generalization of Eq.34 for $\dot{H} \neq 0$.

3.2. False Vacuum Black Hole (BH.fv)

Eq.26 and Eq.27 are the simplest solutions to EFE. They correspond to some form of empty space. The simplest modeling of physical BH interior is a combination of the two:

$$\rho = -p = \begin{cases} 0 & \text{for } r > r_S \\ \Delta & \text{for } r < r_S \end{cases} \tag{35}$$

where $\Delta > 0$. To recover the BH.SW solution outside, we use $V_0 = \Lambda = 0$. The solution to EFE in Eq.24 for Eq.35 (which we called BH.fv) is then:

$$2\Phi = 2\Psi = \begin{cases} -r_S/r & \text{for } r > r_S \equiv 2GM \\ -r^2 H_\Lambda^2 & \text{for } r < r_S = r_\Lambda \equiv 1/H_\Lambda \end{cases} \tag{36}$$

where: $\rho_\Lambda = \rho_{BH} = \Delta$ and $M = \frac{4\pi}{3} r_S^3 \Delta$. Recall that $\Lambda = V_0 = 0$ and ρ_Λ refers to the effective Λ density inside the BH. In a more realistic situation, on larger scales the BH.SW metric should be considered a perturbation of FLRW background, e.g. Eq.21, with $\Lambda \neq 0$ and $V_0 \neq 0$ (see Appendix B).

The above solution has no singularity at $r = 0$. Note how, contrary to what happens in the BH.SW, in the BH.fv solution, the metric components don't change signature as we cross inside r_S. In both sides of r_S we have constant but different values of p and ρ. This comes from energy conservation in Eq.25. There is a discontinuity at $2\Phi = -1$ where $r = r_S$, in agreement with Eq.25, but the metric is static and continuous at r_S. This solution only happens when $r_S = r_\Lambda = (8\pi G\Delta/3)^{-1/2}$. The smaller Δ the larger and more massive the BH. In the limit $\Delta \Rightarrow 0$, we have $r_S = r_\Lambda \Rightarrow \infty$ and we recover Minkowski space, as expected.

At a fixed location, the scalar field φ inside the BH is trapped in a stable configuration ($\rho = V_0 + \Delta$) and can not evolve ($K = 0$ in Eq.9). The same happens for the field outside (see Fig.1). A FV in Eq.35 with equal Δ but with smaller initial radius $r = R < r_S$ is subject to a pressure discontinuity at $r = R$ which is not balanced in Eq.25 and results in a bubble growth ([2, 4]). Such boundary grows and asymptotically reaches $R = r_S$ (see top panel of Fig.3). The inside of r_S is causally disconnected, so the pressure discontinuity does not act on $r = r_S$, which corresponds to a trapped surface.

3.3. FLRW cloud & Black Hole Universe (BH.u)

We next look for solutions where we have matter $\rho_m = \rho_m(t, r)$ and radiation $\rho_R = \rho_R(t, r)$ inside some radius R and empty space outside:

$$\rho(t, r) = \begin{cases} 0 & \text{for } r > R \\ \Delta + \rho_m + \rho_R & \text{for } r < R \end{cases} . \tag{37}$$

When $R > r_S$ we call this a FLRW cloud and when $R < r_S$ this is a BH Universe (BHU of type BH.u). For $r > R$, we have the SW metric. For the interior we use the dSE notation in Eq30: $2\Phi(t, r) \equiv -r^2 H^2(t, r) \equiv -r^2/r_H^2$, so that:

$$2\Phi(t, r) = \begin{cases} -r_S/r & \text{for } r > R \\ -r^2 H^2 & \text{for } r < R \end{cases} \tag{38}$$

At the junction $r = R$, we find that:

$$R = [r_H^2 r_S]^{1/3}, \tag{39}$$

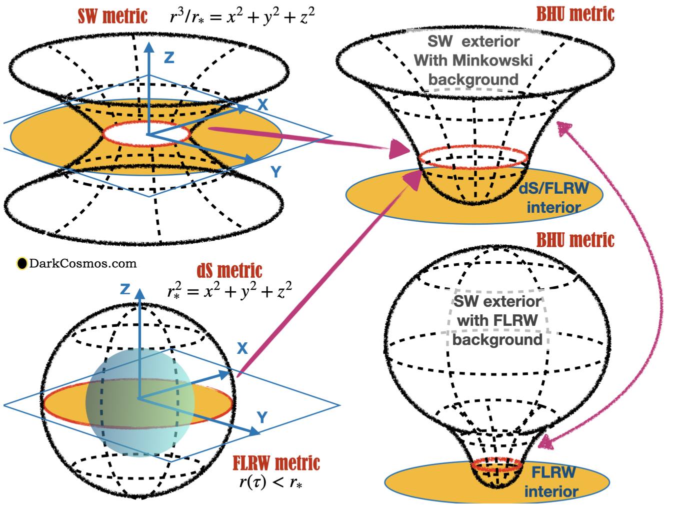

Figure 4: Spatial representation of $ds^2 = (1+2\Phi)^{-1}dr^2 + r^2 d\theta^2$ 2D metric embedded in 3D flat space for: deSitter (dS, bottom left, $2\Phi = -r^2/r_*^2$), FLRW ($r(\tau) < r_*$, blue sphere inside dS), Schwarzschild (SW, top left, $2\Phi = -r_*/r$) and two versions of the combined BHU metrics. Yellow region shows the projection coverage in the (x, y) plane. In the top right figure we show a BHU with dS (or FLRW) interior and SW metric exterior joint at the Event Horizon $r_* = 2GM = 1/H_\Lambda$ (red circles). The BHU solution has in general two nested FLRW metrics join by SW metric (bottom right). See Appendix A for a more detailed explanation.

For $r < R$ we can change variables as in Eq.31-33. In the comoving frame of Eq.33, from every point inside de BHU, comoving observers will have the illusion of an homogeneous and isotropic space-time around them, with a fixed Hubble-Lemaitre expansion $H(\tau)$. This converts dSE metric into FLRW metric. So the solution is $H(t, r) = H(\tau)$ and $R(\tau) = [r_S/H^2(\tau)]^{1/3}$. Given $\rho(\tau)$ and $p(\tau)$ in the interior we can use Eq.14 to find $H(\tau)$ and $R(\tau)$:

$$H^2(\tau) = \frac{8\pi G}{3}\rho(\tau) = \frac{r_S}{R^3(\tau)} \tag{40}$$

This corresponds to a homogeneous FLRW cloud of fix mass $M = r_S/2G$ confined inside $R(\tau)$. The corresponding comoving radius χ_* is $\chi_*(\tau) \equiv R(\tau)/a(\tau)$. We can see how R can be related with a free fall geodesic radial shell:

$$\frac{dR}{d\tau} = a\frac{d\chi_*}{d\tau} + \chi_*\frac{da}{d\tau} = V_0 + HR = V_0 + (r_S/R)^{1/2} \tag{41}$$

where $V_0 \equiv a\dot{\chi}_*$. For a time-like geodesic of constant χ_* ($d\chi = 0$) we have $V_0 = 0$. For a null-like geodesic ($ad\chi = d\tau$): $V_0 = 1$. The later case corresponds to $R = r_*$ in Eq.17 from which we can immediately see that $r_S = r_\Lambda$ like in the BH.fv solution of Eq.36. So even when $\Lambda = \Delta = 0$, the mass M inside R generates $r_\Lambda = r_S$. We will come back to this point in §4.2. We can integrate Eq.41 to find $R(\tau)$, for a fix V_0 and r_S, regardless of $\rho(\tau)$. This shows that a solution for $R(\tau)$ exist for any content inside R.

To complete the solution, i.e. to find Ψ and $\tau = \tau(t, r)$, we need to solve Eq.31 with $2\Phi = -r^2 H^2(\tau)$. For $H(\tau) = H_\Lambda$ the solution is $\Psi = \Phi$ and Eq.34. The FLRW metric with $H = H_\Lambda$ becomes dS metric in Eq.27 as in the BH.fv solution Eq.36. Such solutions are illustrated in Fig.4.

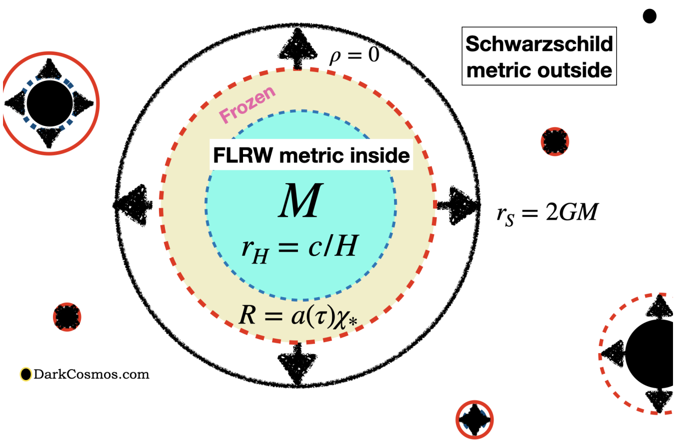

Figure 5: Illustration of the BHU inside the event horizon $r_S = 2GM$. This is a Schwarzschild (empty) metric outside ($r > R$) and a FLRW metric with a Hubble radius $r_H = c/H$ inside ($r < R$). The BHU solution in Eq.39 requires $R = [r_H^2 r_S]^{1/3}$. There is a region with matter outside the Hubble radius $R > r > r_H$ (yellow shading). This solves the horizon problem in Cosmology and is a source for perturbations that enter the horizon as the metric expands, creating LSS and BAO in Cosmic Maps, pretty much like what is usually assumed for Cosmic Inflation.

3.4. *A frozen BH internal layer*

Note how for $R < r_S$ (i.e. inside the BH) Eq.39 indicates that there is a region with no matter: $r_S > r > R$ and a region with matter outside the Hubble horizon $R > r > r_H$. The region increases during collapse inside a BH and re enters the Hubble horizon as it expands. This is a potential source of frozen perturbations, which acts very much like Cosmic Inflation. This is illustrated in Fig.5 (see also Fig.2) and will be further discussed in §6.5

4. Junction conditions

We can arrive at the same BHU (BH.fv and BH.u) solutions using Israel's junction conditions ([52, 53]). We will combine two solutions to EFE with different energy content, as in Eq.37, on two sides (${V_4}^-$ and ${V_4}^+$) of a hypersurface junction $\Sigma = {V_4}^- \cap {V_4}^+$. The inside g^- is FLRW metric and the outside g^+ is BH.SW metric. The junction conditions require that the metric and its derivative (the extrinsic curvature K) match at Σ. This means that the join metric provides a new solution to EFE in $V_4 = {V_4}^-[< \Sigma] \cup {V_4}^+[> \Sigma]$. In many cases, like in the Bubble Universes, this does not work and the junction requires a surface term (the bubble) to glue both solutions together. We will show that for both timelike and null geodesics the junction conditions are satisfied for the BHU and there are no surface terms.

In this section, we follow closely the notation in §12.5 of [31] with $ds^2 = g_{ab}dx^a dx^b$ where $a = 0, 1, 2, 3$ for the 4D metric and $ds^2_\Sigma = h_{\alpha\beta}dy^\alpha dy^\beta$ with $\alpha = 0, 1, 2$ for the 3D induced metric: i.e. ds^2 restricted to the Σ hypersurface.

4.1. *Timelike Junction*

We start by choosing a timelike Σ fixed in comoving coordinates at some value χ_*. This can be identified with a causal boundary, like the free fall collapse of a star of fixed mass M or the particle horizon of Inflation $\chi_\S = \chi_* = (a_i H_i)^{-1}$, where a_i and H_i are the scale factor and Hubble rate when Inflation begins (see §Appendix D). The spherical shell radius follows a radial geodesic trajectory in the FLRW metric. This corresponds to a FLRW cloud of fixed mass M that is expanding or contracting (see also [23] and §12.5 of [31]).

The induced 3D metric $h^-_{\alpha\beta}$ for $dy^\alpha = (d\tau, d\delta, d\theta)$ and fixed $\chi = \chi_*$, is:

$$ds^2_{\Sigma^-} = h^-_{\alpha\beta}dy^\alpha dy^\beta = -d\tau^2 + a^2(\tau)\chi_*^2 d\Omega^2 \tag{42}$$

For the outside SW frame, the junction Σ^+ is described by $r = R(\tau)$ and $t = T(\tau)$, where τ is the FLRW comoving time. We then have:

$$dr = \dot{R}d\tau \;\; ; \;\; dt = \dot{T}d\tau, \tag{43}$$

where the dot refers to derivatives with respect to τ. The metric h^+ induced in the outside SW metric is:

$$\begin{aligned} ds^2_{\Sigma^+} &= h^+_{\alpha\beta}dy^\alpha dy^\beta = -Fdt^2 + \frac{dr^2}{F} + r^2 d\Omega^2 \\ &= -(F\dot{T}^2 - \dot{R}^2/F)d\tau^2 + R^2 d\Omega^2 \end{aligned} \tag{44}$$

where $F \equiv 1 - r_S/R$. Comparing Eq.42 with Eq.44, the first matching conditions $h^- = h^+$ are then:

$$R(\tau) = a(\tau)\chi_* \;\; ; \;\; F\dot{T} = \sqrt{\dot{R}^2 + F} \equiv \beta(R, \dot{R}) \tag{45}$$

For any given $a(\tau)$ and χ_* we can find both $R(\tau)$ and $\beta(\tau)$.

We also want the derivative of the metric to be continuous at Σ. For this, we estimate the extrinsic curvature $K^\pm$ normal to $\Sigma^\pm$ from each side of the hypersurface as:

$$K_{\alpha\beta} = -\left[\partial_a n_b - n_c \Gamma^c_{ab}\right] e^a_\alpha e^b_\beta \tag{46}$$

where $e^a_\alpha = \partial x^a/\partial y^\alpha$ and n_a is the 4D vector normal to Σ. The outward 4D velocity is $u^a = e^a_\tau = (1, 0, 0, 0)$ and the normal to Σ^- on the inside is then $n^- = (0, a, 0, 0)$. On the outside $u^a = (\dot{T}, \dot{R}, 0, 0)$ and $n^+ = (-\dot{R}, \dot{T}, 0, 0)$. It is straightforward to verify that: $n_a u^a = 0$ and $n_a n^a = +1$ (for a timelike surface) for both n^- and n^+.

We then find that the extrinsic curvature in Eq.46 to the Σ junction, estimated with the inside FLRW metric, i.e. K^- is:

$$\begin{aligned} K^-_{\tau\tau} &= -(\partial_\tau n^-_\tau - a\Gamma^\chi_{\tau\tau})e^\tau_\tau e^\tau_\tau = 0 \\ K^-_{\theta\theta} &= a\Gamma^\chi_{\theta\theta}e^\theta_\theta e^\theta_\theta = -a\chi_* = -R \end{aligned} \tag{47}$$

where we have used Eq.45 and the following Christoffel symbols for the FLRW:

$$\begin{aligned} \Gamma^\tau_{\tau\tau} = \Gamma^\tau_{\tau\chi} = \Gamma^\chi_{\tau\tau} = \Gamma^\chi_{\chi\chi} = 0 \;\; &; \;\; \Gamma^\tau_{\theta\theta} = a^2\chi_*^2 H \\ \Gamma^\chi_{\tau\chi} = \Gamma^\tau_{\chi\chi}a^{-2} = H \;\; &; \;\; \Gamma^\chi_{\theta\theta} = -\chi_* \end{aligned} \tag{48}$$

For the SW metric:

$$\begin{aligned} \Gamma^t_{tt} = \Gamma^r_{tr} = 0 \;\; &; \;\; \Gamma^r_{\theta\theta} = -FR\,; \\ \Gamma^t_{tr} = -\Gamma^r_{rr} \;\; &= \;\; \Gamma^r_{tt}F^{-2} = \frac{r_S}{2FR^2} \end{aligned} \tag{49}$$

which results in K^+:

$$\begin{aligned} K^+_{\tau\tau} &= \ddot{R}\dot{T} - \dot{R}\ddot{T} + \frac{\dot{T} r_S}{2R^2 F}(\dot{T}^2 F^2 - 3\dot{R}^2) = \frac{\dot{\beta}}{\dot{R}} \\ K^+_{\theta\theta} &= \dot{T}\Gamma^r_{\theta\theta} = -\dot{T}FR = -\beta R \end{aligned} \tag{50}$$

where we have used the definition of β in Eq.45. In both cases $K_{\delta\delta} = \sin^2\theta K_{\theta\theta}$, so that when $K^-_{\theta\theta} = K^+_{\theta\theta}$ it follows that $K^-_{\delta\delta} = K^+_{\delta\delta}$. Comparing Eq.47 with Eq.50, the matching conditions $K^-_{\alpha\beta} = K^+_{\alpha\beta}$ require $\beta = 1$, which using Eq.45 gives:

$$R = \left[r_H^2 r_S\right]^{1/3} \tag{51}$$

This reproduces the junction in Eq.39. The time equation is:

$$\dot{T} = \frac{1}{1 - R^2 H^2} \tag{52}$$

which is the generalization of Eq.34 for $\dot{H} \neq 0$ and agrees with $\partial_\tau t = (1 + 2\Phi_W)^{-1}$ in Eq.31 for $2\Phi_W = -H^2 R^2$, so it corresponds to a time dilation in the comoving frame.

For constant r_S the timelike Σ, only works for a dust ($p = 0$) matter dominated FLRW metric $r_H^2 \propto a^3$, for only in this case Eq.51 agrees with $R = a\chi_*$ with a constant χ_*. This corresponds to a FLRW dust cloud of fix mass M expanding or collapsing. This case illustrates well the point we want to make. For $p \neq 0$ we need to consider a null junction, which allows for a general $H(\tau)$, see Eq.41 and Appendix C.

4.2. The GHY boundary term

The expansion inside an isolated BH is bounded by the event horizon $r < r_S$ and we need to add the GHY boundary term S_{GHY} to the action in Eq.6, where:

$$S_{GHY} = \frac{1}{8\pi G} \oint_{\partial V_4} d^3y \sqrt{-h}\, K \tag{53}$$

The integral is over the induced metric at ∂V_4, which corresponds to Eq.42, i.e.$\partial V_4 = \Sigma$ at $R = r_S$:

$$ds^2_{\partial V_4} = h_{\alpha\beta} dy^\alpha dy^\beta = -d\tau^2 + r_S^2 d\Omega^2 \tag{54}$$

So the only remaing degrees of freedom in the action are time τ and the angular coordinates. We can use this metric and Eq.47 to estimate K:

$$K = K^\alpha_\alpha = \frac{K_{\theta\theta}}{R^2} + \frac{K_{\delta\delta}}{R^2 \sin^2\theta} = -\frac{2}{R} = -\frac{2}{r_S} \tag{55}$$

We then have

$$S_{GHY} = \frac{1}{8\pi G} \int d\tau\, 4\pi r_S^2\, K = -\frac{r_S}{G}\tau \tag{56}$$

The Λ contribution to the action in Eq.6 is:

$$S_\Lambda = -\frac{\Lambda}{8\pi G} V_4 = -\frac{r_S^3 \Lambda}{3G}\tau \tag{57}$$

We have estimated the total 4D volume V_4 as that bounded by ∂V_4 inside $r < r_S$: $V_4 = 2V_3\tau$, where the factor 2 accounts for the fact that $V_3 = 4\pi r_S^3/3$ is covered twice, first during collapse and again during expansion. Comparing the two terms we can see that we need $\Lambda = 3r_S^{-2}$ or equivalently $r_\Lambda = r_S$ to cancel the boundary term. In other words: evolution inside a BH event horizon induces a Λ term in the EFE even when there is no Λ term to start with. Such event horizon is only a boundary for outgoing geodesics, i.e. expanding solutions. This provides a fundamental interpretation to the observed Λ as a causal boundary [45, 38].

5. The formation of the BHU

How does a BH or our Universe evolve into the solution of Eq.38? This is an important question. It is not enough to find a solution to EFE. We need to make sure that such a configuration can be achieved in a causal way. A good example of this problem is the standard FLRW solution. The FLRW universe has no causal origin: the Hubble rate is the same everywhere, not matter how far, and this is not causally possible ([45, 38]). Cosmic Inflation alleviates this problem, but does not solve it.

We propose here two possible BHU formation scenarios: one that happens during a rapid expansion (or explosion) and a version that happens during the collapse. Both can be applied to a small object, like a star, or a large object, like our Universe. The main difference is that for the larger object the density corresponding to r_S is very low (few atoms per cubic meter) and we can assume a dust ($p = 0$) fluid. This is not the case for small object, like a star. But stars do eventually collapse and explode. Here we focus in formation scenario during collapse which we consider more appealing as it does not require a FV, inflation or DE. In §Appendix D we present the expanding scenario.

5.1. Cloud collapse

Consider a large cloud dominated by dust or CDM (ρ_m with $p = 0$) with radius R and mass M, surrounded by a region of empty space. This is a good approximation for our Universe with $M \simeq 5\times10^{22} M_\odot$ which corresponds to the mass inside our FLRW event horizon r_Λ. The resulting BH density is very low, $\rho_{BH} = 3r_S^{-2}/8\pi G = \rho_\Lambda$, which is 25% lower than the critical density today $\rho = 3H_0^2/8\pi G$ (a few protons per cubic meter). But $p = 0$ is not in always a good approximation. For stellar object $M \simeq M_\odot$ we have $\rho_{BH} \simeq 3M_\odot^{-2}/32\pi G$ corresponds to atomic nuclear density and resist collapse.

Gravity will make such dust cloud collapse following a free fall timelike geodesic of Eq.38 with R given by Eq.51: $R = (r_H^2 r_S)^{1/3}$. As there is no pressure support, it will eventually collapse into a BH when $R = r_S = r_H = 2GM$. The event horizon does not stop the collapse as it only prevents outgoing null geodesics, but it welcomes incoming events. So the collapse continues free fall inside the BH as illustrated in the left half of Fig.6 where the junction $R = (r_H^2 r_S)^{1/3}$ remains valid.

The density increases as $\rho \sim \Delta\tau^{-2}$, where $\Delta\tau$ is the time remaining to reach $R = 0$. As the density inside gets larger it will resist further collapse. The density eventually reaches nuclear atomic density of a neutron star which produces a bounce or

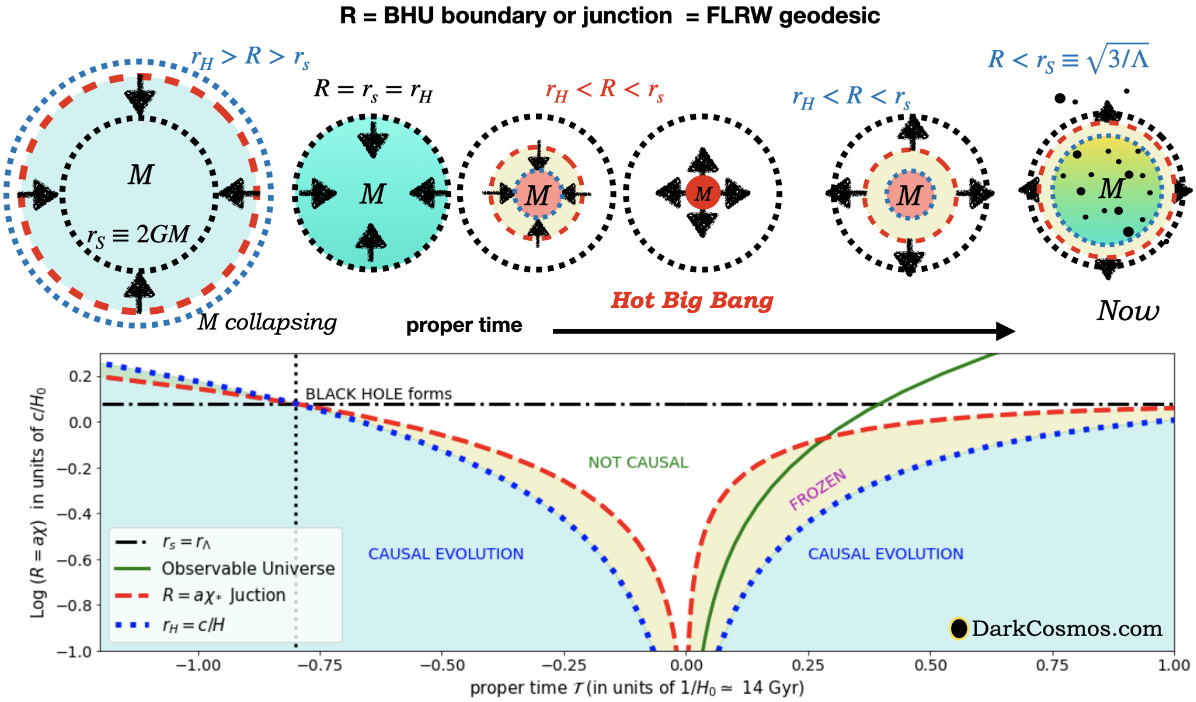

Figure 6: Illustration of the formation of a BHU. A cloud of radius R and mass M collapses under gravity. When it reaches $R = r_S = 2GM$ it becomes a BH. The collapse proceeds inside the BH until it bounces producing an expansion (the hot Big Bang). The event horizon r_S behaves like a cosmological constant with $\Lambda = 3/r_S^2$ so that the expansion freezes before it reaches back to $r_S = r_\Lambda$. The bottom panels shows a numerical calculation for $\Omega_\Lambda = 0.75$ with $R = [r_H^2 r_S]^{1/3}$. Structure in-between R and r_H is frozen and seeds structure formation in our Universe, which could include smaller BHUs, CMB, stars and galaxies.

explosion. This is similar to a supernova explosion or a hot Big Bang. The expansion follows the standard cosmic evolution (nucleosynthesis, CMB decoupling and so on). During radiation domination the junction follows the null geodesic rather the timelike geodesic. The resulting fluid cools down as it expands. Finally it freezes as it reaches back to $R = r_S$.

As detailed in §4.2 the evolution inside a BH event horizon induces a Λ term in the EFE even when there is no Λ term to start with. This provides a fundamental interpretation to the observed Λ as causal boundary [45, 38].

The bottom panel of Fig.6 shows an actual numerical calculation for the formation of our Universe. During collapse, the boundary R is fixed in comoving coordinates and follows $R = [r_H^2 r_S]^{1/3}$, where we have fixed $r_S = 2GM$ to its observed value today $r_S = \Omega_\Lambda^{-1/2}/H_0$ with $\Omega_\Lambda \simeq 0.75$ and r_H is just given by Eq.14 with $\Omega_m \simeq 0.25$ and $\Omega_\Lambda = 0$. After the Big Bang, R follows a null geodesic $ad\chi = d\tau$ (red dashed line) with $H(\tau)$ given by $\Omega_\Lambda \simeq 0.75$ and $\Omega_m \simeq 0.25$. The Big Bang happened $\tau \simeq H_0^{-1} \simeq$ 14Gyrs ago and our Universe collapsed into a BH about 25Gyrs ago.

6. Discusion & Conclusion

Table 1 shows a summary of the notation and models used in this paper. The SW metric in Eq.26 is well known and studied but the interior solution is not physical because it corresponds to a singular point source. Moreover a BH interior can not be made out of regular matter because according to GR an object of mass M must have a minimal radius given by Eq.2 ([8]). What is inside a BH then? We have looked for classical GR solutions for a BH interior. Our motivation is to find a physical model and study if this results in some different observed properties for BHs.

The outside manyfold $V_4{}^+$ of a BH is approximated as empty space so the solution g^+ is the BH.SW metric. Because the inside $V_4{}^-$ is causally disconnected, $V_4{}^+$ acts like a simple boundary condition. Given some ρ and p inside r_S, we can solve EFE inside with such boundary condition to find g^-, the inside metric of a physical BH. We find that g^- is just the well known FLRW. The general solution in Eq.38 corresponds to what we call here a FLRW cloud for $R > r_S$. Such cloud can collapse to become a BHU ($R < r_S$). This solution is not static, which explains how we can avoid the constrain in Eq.2. We have verified Israel´s conditions to double check that the join manyfold $V_4{}^- \cup V_4{}^+$ is also a solution to EFE and there are no surface terms (see §4). This is different from just matching two arbitrary metrics because it correspond to well defined physical content in Eq.37.

The Λ contribution can be interpreted as negative gravity caused by a causal boundary, see §4.2. In the case of our Universe we can interpret the measured r_Λ as the event horizon $r_S = 2GM$ of a large collapsing FLRW cloud of mass M. This sheds new light over the measured coincidence between ρ_Λ and ρ_m [54, 55, 56, 38].

6.1. False Vaccum BH solution (BH.fv)

BH.fv solution corresponds to a constant FV discontinuity (Eq.35) with dS metric inside (Eq.36), with a trapped surface which matches the BH.SW event horizon. A constant density (or negative pressure) corresponds to a centrifugal force, $2\Phi = -(r/r_S)^2$ that opposes Newtonian gravity, $2\Phi = -r_S/r$, i.e. Eq.24. The equilibrium happens when both forces are equal, which fixes $r = r_S$, and is the equivalent of the stable circular Kepler orbits in Newtonian dynamics.

This solution is similar to the classical Bubble Universe solution ([2, 57, 4, 56, 7]) including the gravastar ([10]) and other extensions (e.g. [13, 16, 58, 14, 59]). But there are some important differences. In §4 we show that there are no surface terms. We find that a nullike hypersurface Σ , in Eq.C.5, provides a continuous solution. The same solution is also found in the asymptotic limit $R = r_S$ for a timelike hypersurface Σ of Eq.51.

6.2. The BH universe (BH.u) and FLRW cloud

In Eq.38 we propose a FLRW cloud with a FLRW interior as a solution to GR. When $R < r_S$ this corresponds to a BH.u. We can have other BHs, matter and radiation inside a BHU. The inside needs to be expanding as in the FLRW metric of Eq.11, with a trapped surface given by ρ_Λ. This holds the expansion and balance gravity at r_S as in the BH.fv solution. The join FLRW+SW solution (Eq.38) is also a solution to Einstein's field equations as the two metrics reduce to the same form on a junction (see §4). The junction $R(\tau)$ asymptotically tends to r_S as illustrated by Fig.6.

As with the SW metric, the exterior metric of the BHU could also be FLRW (e.g. see [5] and Eq.21). So in the BHU we have two nested FLRW metrics. This is illustrated in bottom right of Fig.4. We can have smaller BHs inside larger BHs or smaller FLRW metrics inside larger FLRW universes. Mathematically this looks like a Matryoshka (or nesting) doll [19] or a fractal structure [22]. But physically, each BH has a different mass and therefore different physical properties and internal structure.

We have shown in §4.2 that an expanding BH.u interior generates a Λ term even when there is no Λ to start with. If the BHU also contains a true Λ, FV or DE with constant $\rho = \Delta$, the resulting ρ_Λ and the SW radius r_S are

$$8\pi G\rho_\Lambda = 3r_M^{-2} + \Delta \;\; ; \;\; r_S = r_\Lambda = \frac{r_M r_\Delta}{(r_M^2 + r_\Delta^2)^{1/2}} \tag{58}$$

where $r_M = 2GM$ and $r_\Delta = \sqrt{3\Delta/8\pi G}$. In the limit of $\Delta = 0$ we have $r_S = r_M$. For Δ larger than the BH mass density we have $r_S \simeq r_\Delta$. This is similar BH.fv with some subdominant matter and/or radiation inside. The most general BHU would be a combination of both M and Δ.

6.3. BH formation

Another issue, which we address partially in §5 and §Appendix D, is how such physical BHU solutions can be achieved (e.g. astrophysical and primordial BH formation) and if they can have a causal origin. We propose two possible BHU formation scenarios: one that involves FV and can only happen during a rapid expansion (or explosion) and a version that originates in a stellar collapse. Both can be applied to a small object, like a star, or a large object, like our Universe. We have focused in the collapsing case which can result in a BHU without DE or FV. The expanding scenario requires a FV and is presented in §Appendix D. The collapsing scenario is illustrated in Fig.6.

6.4. Our universe as a BH

The BHU can be interpreted as a BH within our universe or as an expanding universe inside a larger space-time. As pointed out in the introduction, that the universe might be generated from the inside of a BH has a long and interesting history. [12] argued that p and ρ in the homogeneous FLRW solution are only a function of time (in comoving coordinates) and can not change at $r = r_S$ to become zero in the exterior. A FLRW cloud collapsing into a BHU allows for an inhomogeneous FLRW solution inside r_S.

Homogeneity is the illusion of the comoving observer inside r_S. The FLRW metric is trapped inside r_* (Eq.17), and is then equivalent to a spherically symmetric metric of Eq.33. The FLRW metric is only homogeneous in space which breaks the relativity principle. The frame duality in Eq.31 is only valid for physical coordinates that are centered at the BH location. But in the transformed (comoving) frame any point inside the BHU is subject to the same expansion law with equal $a(\tau)$. From every point inside de BHU, observers will see an homogeneous and isotropic space-time around them. Just like in the universe around us.

Our observable Universe is consistent with resulting from a collapse of a very large and low density cloud, which we model as a FLRW cloud. As detailed in §5 and Fig.6, such cloud collapsed into a BH. The resulting event horizon is the causal boundary to our Universe and produces the cosmic acceleration that we interpret as DE.

6.5. Is Cosmic Inflation needed?

Inflation ([60, 61, 62, 63]) is an important ingredient in the standard cosmological model. For a review see [64, 65] and also §Appendix D. It solves several problems, the most relevant here are: 1) the horizon problem 2) the source of LSS 3) the flatness problem. The horizon and LSS problems rise because much of the LSS that we observed today, e.g. BAO in CMB maps, was outside the Hubble horizon r_H at the time of light emission and therefore could not have had a causal origin. The idea of inflation is that during the very first instances of the hot Big Bang expansion the Universe became dominated by some FV or DE which produced a dS expansion phase. Such exponential expansion solves all the above problems. But you need to fine tune some mechanisms and potential $V(\varphi)$ to generate a period of slow rolling so that inflation lasted enough e-folds, but stopped at the right time and reheats to allow for the standard expansion that we observed. Such inflation is not directly observable because it occurred when the Universe was opaque.

6.6. The Horizon and LSS problems

As detailed in §3.4 and Fig.5, a large fraction of the mass M that collapsed into our BHU is outside r_H, specially close to the Big Bang phase, as $R = [r_H^2 r_S]^{1/3}$ (see Fig.6). This clearly solves the horizon problem. The same mass outside r_H can be the source of LSS perturbations, such as BAO in Cosmic Maps, as it re-enters r_H. Harrison [66] and Zel'dovich [67] independently proposed in 1970, long before Inflation was invented, that gravitational instability of regular matter alone can generate a scale invariant spectrum of fluctuations, very similar to that in Inflation models.

6.7. The flatness problem

Our results can be extended to models with $k \neq 0$. For example, we reproduce Eq.51 if we define r_H^{-2} to be:

$$r_H^{-2} \equiv H^2 + k/a^2 = \frac{8\pi G}{3}\rho \tag{59}$$

so this does not change our BHU model, interpretation or the expansion/collapse rate. A time-like geodesic of constant comoving radius χ_* contains the same constant mass M also for $k \neq 0$. The flatness problem solved by inflation, is only a problem if we allow for a non flat topology in the FLRW metric. But why choose $k \neq 0$, a donut or a dodecahedron topology for empty space? Given some mass or energy content EFE can not be used to decide the topology of the metric. This is a global property that is either assumed or directly measured. So any choice other than $k = 0$ would require some justification that is outside GR. In our analysis we assumed a global flat topology $k = 0$ because this is the natural choice for empty space.

6.8. Observational test of the BHU

The first evidence for the BHU, as a model for our Universe, is the fact that the measured cosmic density and expansion rate (e.g. r_H) follow Eq.1, which clearly indicates that we live inside a BH. The second evidence comes from measuring cosmic acceleration, which is also an indication of being inside a BH event horizon $r_S = r_\Lambda$. The horizon and LSS problems are also solved in the BHU without need of DE or inflation. Moreover the BHU provides a fundamental model for the meaning of Λ and the hot Big Bang as shown in Fig.6.

The observable Universe today is larger than r_* (the FLRW event Horizon in Fig.2). This indicates that we can observe what happened outside $\chi_* = r_*/a$. At the time of CMB last scattering, χ_* corresponds to an angle $\theta = \chi_*/\chi_o \lesssim 1$ rad $\simeq 60$ deg. So we can actually observe scales larger than χ_*. Scales that are not causally connected! This could be related to the so-called CMB anomalies (i.e, apparent deviations with respect to simple predictions from ΛCDM, see [38, 46, 47] and references therein), or the apparent tensions in measurements from vastly different cosmic scales or times (e.g. [68, 69, 70, 71]).

A measurement of the DE equation of state $\omega \equiv p/\rho \neq -1$ could falsify the BHU. It would indicate that cosmic acceleration is not caused by the causal event horizon r_S produce by M. A possible way around this, is that ω may vary when we include the effect of matter or radiation that is outside the BHU event horizon. If there are other island universes outside ours, Galaxies and QSO, as well as BHs, could have accreted from outside r_S into our BHU. Possible relics around us have been erased during radiation domination. But some relics could have entered after matter domination, in our distant past. If we measured the age of an object (e.g. star, QSO or galaxy) which is older than the BB, this will be a very clear indication in favour of the BHU model. If our universe merged with another BHU which was few % smaller, we might be able to see such % glitches in $H(z)$ with current or future data.

There is good observational evidence for homogeneity and lack of correlations in the CMB at $r > r_\Lambda$ (see [48] and references therein). This suggests that the underlying physical mechanism sourcing the observed anisotropy encompasses scales beyond our causal universe. This agrees with the variations found in cosmological parameters over large CMB regions ([46]), which is the largest reported evidence for a violation of the Cosmological principle. Such observations indicate a breakdown of the standard BB picture, but could be understood within the BHU. Fig.31 in [46] shows that the size of these causal regions follow the BHU relation between $\chi_\S$ and ρ_Λ.

The BHU model allows for a Perfect Cosmologocal Principle, the one advocated by Einstein (when he introduced Λ) and the Steady State Cosmology ([72, 73, 74]). But there is no need for ad hoc matter creation to explain the observed cosmic expansion. The frame duality in Eq.33 explains how we can have at the same time an expanding universe in comoving coordinates (as observed by the Hubble-Lemaitre law) and a static BHU in the outside SW frame.

Acknowledgements

I want to thank Marco Bruni, Robert Caldwell, Ramin G. Daghigh, Alberto Diez-Tejedor and Angela Olinto, for their feedback. This work has been supported by spanish MINECO grants PGC2018-102021-B-100 and EU grants LACEGAL 734374 and EWC 776247 with ERDF funds. IEEC is funded by the CERCA program of the Generalitat de Catalunya.

Appendix A. Geometrical representations

To visualize the BHU metric in a 2D plot we consider the most general shape for a spherically symmetric metric in 2D space (x, y) embedded in 3D flat space (x, y, z) (see also §7.1.3 in [31]). In polar coordinates (r, θ) with $r^2 = x^2 + y^2$ and $\tan\theta = x/y$ we have:

$$ds^2 = \frac{dr^2}{1 + 2\Phi} + r^2 d\theta^2 \tag{A.1}$$

In 3D space we just have one additional angle, δ, in Eq.19, but the radial part is the same. The case $\Phi = 0$ corresponds to flat space: $ds^2 = dx^2 + dy^2$. The simplest case with curvature can be represented by a 2D sphere (S2) embedded in 3D flat space using an extra dimension z:

$$ds^2 = dx^2 + dy^2 + dz^2 \quad ; \quad x^2 + y^2 + z^2 = r_*^2 \tag{A.2}$$

This metric is flat in 3D coordinates, but constraint to r_*, which is the radius of the sphere and the curvature within the 2D surface of S2. We can replace z by r using: $z^2 = r_*^2 - r^2$ to find:

$$ds^2 = dx^2 + dy^2 + dz^2 = \frac{dr^2}{1 - r^2/r_*^2} + r^2 d\theta^2 \quad \text{(A.3)}$$

so that $2\Phi = -r^2/r_*^2$ just like in the dS metric of Eq.27 for $r_* = r_\Lambda$. It tell us that dS space corresponds to being in the flat surface of a sphere (like us in Earth). This is illustrated in the bottom left of Fig.4. Note how (r, θ) are coordinates in the (x, y) plane. The S2 space is trapped or bounded by $r < r_*$ (yellow region). The metric changes signature (becomes imaginary) for $r > r_*$: this region can't be reached (white region). The case $r = r_*$ (red circles) corresponds to the Event Horizon at $2\Phi = -1$.

The Newtonian interpretation of $2\Phi = -r^2/r_*^2$ is that this is caused by a centrifugal force, like that in the orbit of a satellite. Even when there is no matter, the curvature (or boundary) is interpret as a repulsive gravitational force that causes acceleration.

The FLRW metric (or dSE metric in Eq.33) correspond to a smaller sphere S2 (inside dS sphere) with an expanding radius $r_H(\tau)$ that tends asymptotically to $r_\Lambda = 1/H_\Lambda$ (see Eq.33):

$$ds^2 = dx^2 + dy^2 + dz^2 \quad ; \quad x^2 + y^2 + z^2 = r_H^2(\tau) \quad \text{(A.4)}$$

So it has the same topology and Event Horizon or trapped surface (red circle) as dS metric. It is represented in Fig.4 by a blue sphere inside dS sphere in the bottom left corner. This illustrates how it is possible that each observer inside sees an homogeneous space even when the sphere is centered around a given position.

The next simplest case can be represent by a static radius that increases with r, i.e. : $x^2 + y^2 + z^2 = r^3/r_*$. We can replace z by r using: $z^2 = r^3/r_* - r^2$ to find:

$$ds^2 = dx^2 + dy^2 + dz^2 = \frac{dr^2}{1 - r_*/r} + r^2 d\theta^2 \quad \text{(A.5)}$$

so that $2\Phi = -r_*/r$ just like in the SW metric of Eq.26 for $r_* = 2GM$. This is illustrated in the top left of Fig.4. The case $r = r_*$ (red circle) corresponds to the Event Horizon at $2\Phi = -1$. The Newtonian interpretation for $2\Phi = -r_*/r$ is the inverse square law for a point mass M: $r_* = 2GM$.

The SW space is bounded by $r > r_*$ (yellow region). The metric changes signature (becomes imaginary) for $r < r_*$ and this region can not be reached. This coverage is complementary to dS or FLRW metric which only cover the inner region. We can match the dS and SW metrics at $r = r_*$ to cover the full (x, y) plane as in the BHU metric. Physically this corresponds to a balance between the centrifugal force, represented by dS potential $2\Phi = -r^2/r_*$, and the SW inverse square law, $2\Phi = -r_*/r$, like what happens in the circular Keplerian orbits. This matching is the junction in Eq.51 which corresponds to a causal boundary. This can also be seem as a Lorentz contraction $\gamma = 1/\sqrt{1-u^2}$ where the velocity u is given by the Hubble-Lemaitre law: $u = Hr$. The time duality between the FLRW and SW frame can also be interpreted as a time dilation, see Eq.33.

This BHU metric is shown in the top right of Fig.4, which is asymptotically Minkowski. The dS metric is the limiting case of FLRW metric and SW metric is a perturbation over FLRW metric. So more generally, the BHU is a combination of 2 FLRW metrics join by a SW metric. The junction happens at the effective value of $r_* = r_\Lambda = 2GM$ corresponding to the inner FLRW ρ_Λ (which we denote as ρ_{Λ_-}). If the outer FLRW has $\rho_{\Lambda_+} \neq 0$, then the SW hyperbolic surface will close as another S2 sphere (bottom right).

Appendix B. Non empty solution

Eq.35 for $V_0 \neq 0$ and $\Lambda \neq 0$:

$$\rho(r) = \begin{cases} V_0 & \text{for } r > r_S \\ V_0 + \Delta & \text{for } r < r_S \end{cases} \quad \text{(B.1)}$$

can be solved as $\Phi = \Psi$ with

$$2\Phi = \begin{cases} -r_S/r - r^2 H_{\Lambda_+}^2 & \text{for } r > r_S \equiv 2GM(1+\epsilon) \\ -r^2 H_{\Lambda_-}^2 & \text{for } r < r_S = r_{\Lambda_-} \equiv 1/H_{\Lambda_-} \end{cases} \quad \text{(B.2)}$$

where $\epsilon \equiv \rho_{\Lambda_+}/\Delta$ and

$$3H_{\Lambda_+}^2 \equiv 8\pi G \rho_{\Lambda_+} \quad ; \quad \rho_{\Lambda_+} = \Lambda/8\pi G + V_0 \quad \text{(B.3)}$$

$$3H_{\Lambda_-}^2 \equiv 8\pi G \rho_{\Lambda_-} \quad ; \quad \rho_{\Lambda_-} = \rho_{\Lambda_+} + \Delta \quad \text{(B.4)}$$

So there are different effective ρ_Λ outside (ρ_{Λ_+}) and inside (ρ_{Λ_-}), but only one Λ. The exterior of the BH has the dSW metric but more generally it is a perturbation of the FLRW metric.

Appendix C. Null Junction

A null junction has degeneracies which requires more elaborate consideration. This level of detail is beyond the scope of this paper, so we only give a brief account of such calculation. For a more careful analysis see [53]. We choose Σ to be a radial null surface in the FLRW metric, i.e.: $d\tau = a d\chi$. This results in a radial coordinate $\chi_*(\tau)$ which is no longer constant and that we want to identify with the FLRW event horizon of Eq.17. At any given time the corresponding physical distance is $r_*(\tau) = a(\tau)\chi_*(\tau)$ with $\dot{\chi}_* = 1/a$. For the outside SW coordinate system, Σ^+ is described as before by Eq.43. The induced inside metric h^- with $y^\alpha = (\tau, \theta, \delta)$ and $d\tau = a d\chi$ is now:

$$h_{\alpha\beta}^- dy^\alpha dy^\beta = a^2 \chi_*^2 d\Omega^2 = r_*^2(\tau) \left[d\theta^2 + \sin^2(\theta) d\delta^2 \right] \quad \text{(C.1)}$$

This has to agree with h^+ in Eq.44. The first matching conditions $h^- = h^+$ are in this case:

$$R = r_*(\tau) = a\chi_* \quad \Rightarrow \quad \dot{R} = 1 + HR \quad \text{(C.2)}$$

$$F^2 \dot{T}^2 = \dot{R}^2 \quad \Rightarrow \quad \dot{T} = \frac{\dot{R}}{1 - r_S/R} \quad \text{(C.3)}$$

The outward 4D velocity is $u^a = e_t^a = (1, 1/a, 0, 0)$, so it has a radial component in the comoving frame. For a null surface we define a transverse extrinsic curvature [53]. We use the same notation as in Eq.46 with the difference that n is now a transverse null vector: $n_a u^a = 0$ and $n_a n^a = 0$. We then have: $n^- = A(1, -a, 0, 0)$ where $A = A(\tau)$ is an arbitrary function of τ. On the outside $u^a = (\dot{T}, \dot{R}, 0, 0)$ and $n^+ = (-\dot{R}, \dot{T}, 0, 0)$ as before, but where we have now used the new matching condition above $\dot{R} = F\dot{T}$ in Eq.C.3. Using the Christoffel symbols in Eq.48 and Eq.49, we find:

$$\begin{aligned} K^-_{\tau\tau} &= -\partial_\tau n^-_\tau - 2A\Gamma^\chi_{\tau\chi} - \frac{1}{a}\partial_\tau n^-_\chi - \frac{A}{a^2}\Gamma^\tau_{\chi\chi} = 0 \\ K^+_{\tau\tau} &= \ddot{R}\dot{T} - \dot{R}\ddot{T} + \frac{\dot{T} r_S}{2R^2 F}(\dot{T}^2 F^2 - 3\dot{R}^2) = 0 \\ K^-_{\theta\theta} &= A\Gamma^\tau_{\theta\theta} - aA\Gamma^\chi_{\theta\theta} = AR(HR - 1) \\ K^+_{\theta\theta} &= \dot{T}\Gamma^r_{\theta\theta} = -\dot{T}FR = -\dot{R}R \\ K^\pm_{\delta\delta} &= \sin^2\theta\, K^\pm_{\theta\theta} \end{aligned} \tag{C.4}$$

Thus, the second matching conditions $K^-_{\alpha\beta} = K^+_{\alpha\beta}$ together with Eq.C.2 results in:

$$\dot{R} = 1 + HR \quad ; \quad A = \frac{1 + HR}{1 - HR} \tag{C.5}$$

The left hand side is fulfil for any $H(\tau)$ as long as $R = a\chi_*$ is a null geodesic (i.e $\dot{\chi}_* = 1/a$), which is our staring point in Eq.C.2 and agrees with Eq.41 for $V_0 = 1$. The right hand side fixes the normalization $A = A(\tau)$ of n^- in Σ^-.

When a is small the null geodesics $R = r_*$ in the integral of Eq.17 is dominated by the late time value of H_Λ and this means that the FLRW event horizon χ_* is fixed in comoving coordinates. This reproduces the junction in Eq.51. On the opposite limit, when H is constant: $H = H_\Lambda = r_\Lambda^{-1}$ we have $\dot{R} = 0$ and $R = r_\Lambda = r_H = r_S$. This results in $2\Psi = 2\Phi = -H^2R^2 = -r_S/R = -1$ in the junction Σ, as in the BH.fv solution of Eq.36. This makes sense because for a dS expansion null events are fixed in physical coordinates.

Appendix C.1. The GHY boundary term

We estimate the GHY boundary term to the action S_{GHY} following the steps in §4.2. We use the formalism in [75] for boundaries of null surfaces. This is similar to what we did before with the main difference that the induced metric is now 2D instead of 3D:

$$ds^2 = q_{AB} dz^A dz^B = R^2(d^2\theta + \sin^2\theta d\delta^2). \tag{C.6}$$

and

$$S_{GHY} = \frac{1}{8\pi G}\oint_{\partial V_4} d\lambda d^2 z_\perp \sqrt{q}\,(\Theta + \kappa) \tag{C.7}$$

where κ is the non-affinity coefficient: $l^a\nabla_a l_b = \kappa l_b$ and

$$\Theta \equiv q^{AB}\Theta_{AB} = \frac{K_{\theta\theta}}{R^2} + \frac{K_{\delta\delta}}{R^2\sin^2\theta} \tag{C.8}$$

We can use Eq.C.4 to find $\Theta = -2\dot{R}/R = -2\kappa$. So the corresponding trace of the extrinsic curvature is:

$$\Theta + \kappa = -\frac{\dot{R}}{R} \tag{C.9}$$

For ∂V_4 we have $R = r_S$ and $\dot{R} = 2$. Thus, we recover the same result as Eq.55. From this we can arrive to the same conclusion that the boundary GHY term fixes $r_\Lambda = r_S$.

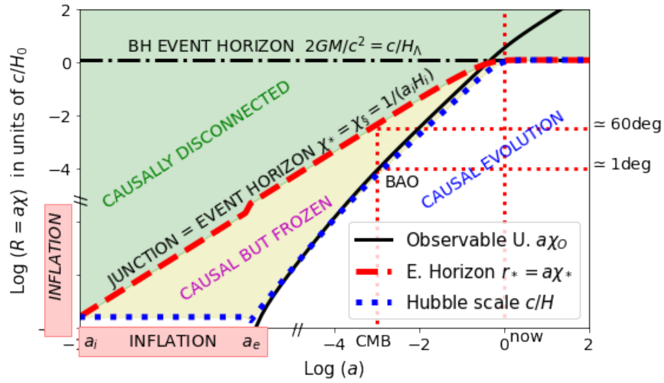

Figure D.7: Extension of Fig.2 to the period of inflation. The FLRW Event Horizon $r_* = a\chi_*$ in Eq.17 (red dashed line) here is also the BHU junction and matches the primordial causal boundary for inflation $\chi_* = \chi_\S$. Scales larger than r_* are causally disconnected (green shading). Our event horizon today $a\chi_* \simeq c/H_\Lambda$ becomes the BH event horizon (dot-dashed line) in the SW frame.

Appendix D. Forming a BHU in an expanding background

To form a BHU during an explosion or rapid expansion we need a FV, ρ_Λ, term as explained in §2.1. This will play the role of Dark Energy (DE). Consider a localized field with some fixed total energy $\rho = K + V$ (black dot labeled ρ_5 in Fig.1). In an expanding background (such a supernovae explosion or Inflation) the field can rapidly lose its kinetic energy (K_5), due to Hubble damping, and end up trapped inside some FV (V_5). If the outside background is at a lower FV, this will generate an expanding BH of type BH.fv, as discussed in §3.2. This could be the start of some inflation. Because additional FV structure can exist within a given FV, the same Hubble damping can form a BH.fv inside a larger BH.fv. When K is not fully damped, the classical reheating mechanism around a FV could also be a source of matter/radiation. This could turn a BH.fv into BH.u (see §3.3). There is some literature on Bubble Universe formation (e.g. see [56, 14] and references therein) but they typically involve quantum gravity ideas or GR extensions. As illustrated in Fig.1 there could be a landscape of nested BHU of different masses and sizes. The masses and sizes of such BH.fv bares no relation with the energy of the expansion (e.g. supernova explosion or inflation) or the host object which originated the expansion. Such BHUs are similar to primordial BHs [7].

A possible evolution of our universe is shown in Fig.D.7. The Hubble Horizon r_H is defined as $r_H = c/H$. Scales larger than r_H cannot evolve because the time a perturbation takes to travel that distance is larger than the expansion time. This means that $r > r_H$ scales are "frozen out" (structure can not evolve) and are causally disconnected from the rest (e.g. see [65]). Thus, c/H represents a dynamical causal horizon that is evolving. This was illustrated in Fig.2 and Fig.5.

A primordial field φ settles or fluctuates into a false (or slow rolling) vacuum which will create a BH.fv with null junction Σ in Eq.C.2. Such causal boundary to the particle horizon during inflation $\chi_\S = c/(a_i H_i)$ or the Hubble horizon when inflation begins. The size $R = a(\tau)\chi_\S$ of this vacuum grows and asymptotically tends to $r_H = c/H$ with $H = H_i$. The inside of this

BH will be expanding exponentially $a = e^{\tau H_i}$ while the Hubble horizon is fixed $1/H_i$. Accoording to standard models of primordial inflation ([60, 61, 62, 63]), this inflation ends (at some a_e) and vacuum energy excess converts into matter and radiation (reheating). This results in BH.u, where the infinitesimal Hubble horizon starts to grow following the standard BB evolution. Note that the inflation in the BH.fv solution stops naturally at cosmic time $\tau_i = -H_i^{-1} \ln \chi_{\S} H_i$ (see Fig.3) when physical SW distance is $r = a(\tau)\chi_{\S} = 1/H_i$. In standard models of primordial inflation, H_i is much larger that H_Λ so that $1/H_i$ is much smaller than $1/H_\Lambda$. So a FV Δ only grows to a maximum size $R = r_S = (8\pi G\Delta/2)^{-1/2} = 1/H_i$. Something else has to happen if we want the size to become cosmological. In inflation this is provided by slow rolling. Regardless of these formation details, $\chi_{\S}$ remains the causal scale for the original BH.fv inflation, unless slow rolling ends before. So we propose to identify χ_* in Eq.C.2 with $\chi_{\S}$ from inflation (see also Fig.2) which is equivalent to say that DE is just inflation.

Smaller primordial BH could be created following similar scenarios within the expansion caused by Cosmic Inflation or during a SN explosion. The size of the BHU will depend on the combination of ρ_Λ and the slow rolling mechanism. For such BH.fv it seems that any matter falling inside will be diluted away by the rapid internal expansion and will not affect its size.

References

[1] N. Dadhich, Singularity: Raychaudhuri equation once again, Pramana 69 (1) (2007) 23. arXiv:gr-qc/0702095, doi:10.1007/s12043-007-0108-3.

[2] S. K. Blau, E. I. Guendelman, A. H. Guth, Dynamics of false-vacuum bubbles, PRD 35 (6) (1987) 1747–1766. doi:10.1103/PhysRevD.35.1747.

[3] P. O. Mazur, E. Mottola, Gravitational Condensate Stars: An Alternative to Black Holes, arXiv e-prints (2001) gr–qc/0109035arXiv:gr-qc/0109035.

[4] A. Aguirre, M. C. Johnson, Dynamics and instability of false vacuum bubbles, PRD 72 (10) (2005) 103525. doi:10.1103/PhysRevD.72.103525.

[5] N. Kaloper, M. Kleban, D. Martin, McVittie's legacy: Black holes in an expanding universe, PRD 81 (10) (2010) 104044. doi:10.1103/PhysRevD.81.104044.

[6] J. Kormendy, L. C. Ho, Coevolution (Or Not) of Supermassive Black Holes and Host Galaxies, ARAA 51 (1) (2013) 511–653. arXiv:1304.7762, doi:10.1146/annurev-astro-082708-101811.

[7] A. e. Kusenko, Exploring Primordial Black Holes from the Multiverse with Optical Telescopes, PRL 125 (18) (2020) 181304. arXiv:2001.09160, doi:10.1103/PhysRevLett.125.181304.

[8] H. A. Buchdahl, General relativistic fluid spheres, Phys. Rev. 116 (1959) 1027–1034. doi:10.1103/PhysRev.116.1027.
URL https://link.aps.org/doi/10.1103/PhysRev.116.1027

[9] R. Brustein, A. J. M. Medved, Resisting collapse, PRD 99 (6) (2019) 064019. doi:10.1103/PhysRevD.99.064019.

[10] P. O. Mazur, E. Mottola, Surface tension and negative pressure interior of a non-singular 'black hole', Classical and Quantum Gravity 32 (21) (2015) 215024. doi:10.1088/0264-9381/32/21/215024.
URL https://doi.org/10.1088/0264-9381/32/21/215024

[11] P. T. Landsberg, Mass Scales and the Cosmological Coincidences, Annalen der Physik 496 (2) (1984) 88–92. doi:10.1002/andp.19844960203.

[12] H. Knutsen, The idea of the universe as a black hole revisited, Gravitation and Cosmology 15 (3) (2009) 273–277. doi:10.1134/S0202289309030128.

[13] D. A. Easson, R. H. Brandenberger, Universe generation from black hole interiors, J. of High Energy Phy. 2001 (6) (2001) 024. doi:10.1088/1126-6708/2001/06/024.

[14] N. Oshita, J. Yokoyama, Creation of an inflationary universe out of a black hole, Physics Letters B 785 (2018) 197–200. doi:10.1016/j.physletb.2018.08.018.

[15] G. Ellis, J. Silk, Scientific method: Defend the integrity of physics, Nature 516 (7531) (2014) 321–323. doi:10.1038/516321a.

[16] R. G. Daghigh, J. I. Kapusta, Y. Hosotani, False Vacuum Black Holes and Universes, arXiv:gr-qc/0008006 (Aug. 2000).

[17] D. V. Galtsov, J. P. Lemos, No-go theorem for false vacuum black holes, Classical and Quantum Gravity 18 (9) (2001) 1715–1726. arXiv:gr-qc/0008076, doi:10.1088/0264-9381/18/9/308.

[18] I. Dymnikova, Spherically Symmetric Space Time with Regular de Sitter Center, International Journal of Modern Physics D 12 (6) (2003) 1015–1034. arXiv:gr-qc/0304110, doi:10.1142/S021827180300358X.

[19] R. K. Pathria, The Universe as a Black Hole, Nature 240 (5379) (1972) 298–299. doi:10.1038/240298a0.

[20] I. J. Good, Chinese universes, Physics Today 25 (7) (1972) 15. doi:10.1063/1.3070923.

[21] N. Popławski, Universe in a Black Hole in Einstein-Cartan Gravity, ApJ 832 (2) (2016) 96. arXiv:1410.3881, doi:10.3847/0004-637X/832/2/96.

[22] T. X. Zhang, The Principles and Laws of Black Hole Universe, Journal of Modern Physics 9 (9) (2018) 1838–1865. doi:10.4236/jmp.2018.99117.

[23] W. M. Stuckey, The observable universe inside a black hole, American Journal of Physics 62 (9) (1994) 788–795. doi:10.1119/1.17460.

[24] L. Smolin, Did the universe evolve?, Classical and Quantum Gravity 9 (1) (1992) 173–191. doi:10.1088/0264-9381/9/1/016.

[25] G. Ellis, Opposing the multiverse, Astronomy and Geophysics 49 (2) (2008) 2.33–2.35. doi:10.1111/j.1468-4004.2008.49229_1.x.

[26] L. Dyson, M. Kleban, L. Susskind, Disturbing Implications of a Cosmological Constant, J.of High Energy Phy 2002 (10) (2002) 011. arXiv:hep-th/0208013, doi:10.1088/1126-6708/2002/10/011.

[27] R. Penrose, Before the big bang: An outrageous new perspective and its implications for particle physics, Conf. Proc. C 060626 (2006) 2759–2767.

[28] D. Hilbert, Die Grundlage der Physick, Konigl. Gesell. d. Wiss. Göttingen, Math-Phys K 3 (7) (1915) 395–407. doi:10.1002/andp.19163540702.

[29] S. Weinberg, Gravitation and Cosmology, John Wiley & Sons, NY, 1972.

[30] S. Weinberg, Cosmology, Oxford University Press, 2008.

[31] T. Padmanabhan, Gravitation, Cambridge Univ. Press, 2010.

[32] A. Einstein, Die Grundlage der allgemeinen Relativitätstheorie, Annalen der Physik 354 (7) (1916) 769–822. doi:10.1002/andp.19163540702.

[33] L. D. Landau, E. M. Lifshitz, The classical theory of fields, 1971.

[34] S. M. Carroll, Spacetime and geometry. Addison-Wesley,, 2004.

[35] J. W. York, Role of Conformal Three-Geometry in the Dynamics of Gravitation, PRL 28 (16) (1972) 1082–1085. doi:10.1103/PhysRevLett.28.1082.

[36] G. W. Gibbons, S. W. Hawking, Cosmological event horizons, thermodynamics, and particle creation, PRD 15 (10) (1977) 2738–2751. doi:10.1103/PhysRevD.15.2738.

[37] S. W. Hawking, G. T. Horowitz, The gravitational Hamiltonian, action, entropy and surface terms, Class Quantum Gravity 13 (6) (1996) 1487–1498. arXiv:gr-qc/9501014, doi:10.1088/0264-9381/13/6/017.

[38] E. Gaztañaga, The cosmological constant as a zero action boundary, MNRAS 502 (1) (2021) 436–444. doi:10.1093/mnras/stab056.

[39] J. García-Bellido, L. Espinosa-Portalés, Cosmic acceleration from first principles, Physics of the Dark Universe 34 (2021) 100892. arXiv:2106.16014, doi:10.1016/j.dark.2021.100892.

[40] L. Espinosa-Portalés, J. García-Bellido, Covariant formulation of non-equilibrium thermodynamics in General Relativity, Physics of the Dark Universe 34 (2021) 100893. doi:10.1016/j.dark.2021.100893.

[41] R. Arjona, L. Espinosa-Portales, J. García-Bellido, S. Nesseris, A GREAT model comparison against the cosmological constant, arXiv e-prints (2021) arXiv:2111.13083arXiv:2111.13083.

[42] A. Diez-Tejedor, A. Feinstein, Homogeneous scalar field the wet dark sides of the universe, PRD 74 (2) (2006) 023530. doi:10.1103/PhysRevD.74.023530.

[43] G. F. R. Ellis, T. Rothman, Lost horizons, American Journal of Physics 61 (10) (1993) 883–893. doi:10.1119/1.17400.

[44] S. Deser, J. Franklin, Schwarzschild and Birkhoff a la Weyl, American Journal of Physics 73 (3) (2005) 261–264. arXiv:gr-qc/0408067, doi:10.1119/1.1830505.
[45] E. Gaztañaga, The size of our causal Universe, MNRAS 494 (2) (2020) 2766–2772. doi:10.1093/mnras/staa1000.
[46] P. Fosalba, E. Gaztañaga, Explaining cosmological anisotropy: evidence for causal horizons from CMB data, MNRAS 504 (4) (2021) 5840–5862. arXiv:2011.00910, doi:10.1093/mnras/stab1193.
[47] E. Gaztañaga, P. Fosalba, A peek outside our Universe (2021) arXiv:2104.00521.
[48] B. Camacho, E. Gaztañaga, A measurement of the scale of homogeneity in the Early Universe, arXiv e-prints (2021) arXiv:2106.14303arXiv:2106.14303.
[49] K. Lanczos, Bemerkung zur de Sitterschen Welt, Phys.Z. 23 (24) (1922) 539–543. doi:10.1002/andp.19163540702.
[50] A. Mitra, Interpretational conflicts between the static and non-static forms of the de Sitter metric, Nature Sci. Reports 2 (2012) 923. doi:10.1038/srep00923.
[51] K. Lanczos, C. Hoenselaers, On a Stationary Cosmology in the Sense of Einstein's Theory of Gravitation [1923], GR and Gravitation 29 (1997) 361–399.
[52] W. Israel, Singular hypersurfaces and thin shells in general relativity, Nuovo Cimento B Serie 48 (2) (1967) 463–463. doi:10.1007/BF02712210.
[53] C. Barrabès, W. Israel, Thin shells in general relativity and cosmology: The lightlike limit, PRD 43 (4) (1991) 1129–1142. doi:10.1103/PhysRevD.43.1129.
[54] S. Weinberg, The cosmological constant problem, Reviews of Modern Physics 61 (1) (1989) 1–23. doi:10.1103/RevModPhys.61.1.
[55] P. J. Peebles, B. Ratra, The cosmological constant and dark energy, Reviews of Modern Physics 75 (2) (2003) 559–606. arXiv:astro-ph/0207347, doi:10.1103/RevModPhys.75.559.
[56] J. Garriga, A. Vilenkin, J. Zhang, Black holes and the multiverse, JCAP 2016 (2) (2016) 064. arXiv:1512.01819, doi:10.1088/1475-7516/2016/02/064.
[57] V. P. Frolov, M. A. Markov, V. F. Mukhanov, Through a black hole into a new universe?, Phys Let B 216 (3-4) (1989) 272–276. doi:10.1016/0370-2693(89)91114-3.
[58] H. Firouzjahi, Primordial Universe Inside the Black Hole and Inflation, arXiv e-prints (2016) arXiv:1610.03767.
[59] I. Dymnikova, Universes Inside a Black Hole with the de Sitter Interior, Universe 5 (5) (2019) 111. doi:10.3390/universe5050111.
[60] A. A. Starobinskiǐ, Spectrum of relict gravitational radiation and the early state of the universe, Soviet J. of Exp. and Th. Physics Letters 30 (1979) 682.
[61] A. H. Guth, Inflationary universe: A possible solution to the horizon and flatness problems, PRD 23 (2) (1981) 347–356. doi:10.1103/PhysRevD.23.347.
[62] A. D. Linde, A new inflationary universe scenario, Physics Letters B 108 (6) (1982) 389–393. doi:10.1016/0370-2693(82)91219-9.
[63] A. Albrecht, P. J. Steinhardt, Cosmology for Grand Unified Theories with Radiatively Induced Symmetry Breaking, PRL 48 (17) (1982) 1220–1223. doi:10.1103/PhysRevLett.48.1220.
[64] A. R. Liddle, Observational tests of inflation, arXiv e-prints (1999) astro–ph/9910110arXiv:astro-ph/9910110.
[65] S. Dodelson, Modern cosmology, Academic Press, NY, 2003.
[66] E. R. Harrison, Fluctuations at the Threshold of Classical Cosmology, PRD 1 (10) (1970) 2726–2730. doi:10.1103/PhysRevD.1.2726.
[67] Y. B. Zel'Dovich, Reprint of 1970A&A.....5...84Z. Gravitational instability: an approximate theory for large density perturbations., AAP 500 (1970) 13–18.
[68] Planck Collaboration, Planck 2018 results. VI. Cosmological parameters, A&A 641 (2020) A6. doi:10.1051/0004-6361/201833910.
[69] A. G. Riess, The expansion of the Universe is faster than expected, Nature Reviews Physics 2 (1) (2019) 10–12. doi:10.1038/s42254-019-0137-0.
[70] DES Collaboration, Cosmological Constraints from Multiple Probes in the Dark Energy Survey, PRL 122 (17) (2019) 171301. arXiv:1811.02375, doi:10.1103/PhysRevLett.122.171301.
[71] E. Di Valentino, O. Mena, S. Pan, L. Visinelli, W. Yang, A. Melchiorri, D. F. Mota, A. G. Riess, J. Silk, In the realm of the Hubble tension-a review of solutions, Classical and Quantum Gravity 38 (15) (2021) 153001. arXiv:2103.01183, doi:10.1088/1361-6382/ac086d.
[72] C. O'Raifeartaigh, S. Mitton, A new perspective on steady-state cosmology (2015) arXiv:1506.01651.
[73] H. Bondi, T. Gold, The Steady-State Theory of the Expanding Universe, MNRAS 108 (1948) 252. doi:10.1093/mnras/108.3.252.
[74] F. Hoyle, A New Model for the Expanding Universe, MNRAS 108 (1948) 372. doi:10.1093/mnras/108.5.372.
[75] K. Parattu, S. Chakraborty, B. R. Majhi, T. Padmanabhan, A boundary term for the gravitational action with null boundaries, General Relativity and Gravitation 48 (7) (2016) 94. arXiv:1501.01053, doi:10.1007/s10714-016-2093-7.